



value it is necessary to reduce the magnitude of the total magnetic flux. This can be achieved by means of current in the longitudinal  $d$ -axis, which will form the flux of the opposite direction than the flux of the PM. Since the rated current cannot be exceeded for a longer time interval because of the cooling of the machine, the torque component of the current has to be reduced as well, which leads to the quick decrease of the torque developed with the speed.

The control structure is formed by so-called subordinate control loops consisting of one or more simple controllers (see Fig.1). Because of the reduction of the number of controllers and elimination of alternate quantities the space vectors consisting of three phases are converted into a rotary two-component system. For PMSM it is most suitable to use the rotating coordinate system oriented on the magnetic flux of the PM. In this coordinate system the quantities are direct in the steady state. So as to ensure the maximum dynamics it is necessary to force the torque current into the stator winding within the shortest possible time. The delay between the controlled and the required values of current corresponds to the non-compensated time constant of the current loop.

### Sensorless control methods of PMSM

The term sensorless control means elimination of the rotor position sensor or speed sensor, i.e. sensors for mechanical quantities located on the machine shaft. Sensorless methods use many different principles. These methods usually processed stator voltages and currents. Methods based on artificial intelligence, i.e. artificial neural networks and fuzzy logic could be included in the category of the most sophisticated systems [5, 6, 7].

More common sensorless methods are methods working with the mathematical model of machines or injection methods.

The mathematical model of a machine describes the behaviour of the machine in dependence on the supply voltage and on the load torque. For simplicity the mathematical model ignores many actual properties of electric machines. This affects the accuracy of the mathematical description and limits its use. There are many mathematical models on which a lot of more specific methods are based, such as MRAS, various types of observers, integration methods, Kalman filter etc. [8]-[17].

From the view of state values the counter-voltage and magnetic flux can primarily be used for the estimation. The counter-voltage can be estimated by using an observer; the integration approach is typical for magnetic fluxes. Usually the stator current and voltage vectors are used as the input data for the estimation. If the neutral wire is not led out of the machine, it is possible to measure the currents of two phases and calculate the third one. The easiest way to get the stator voltage is to obtain it from the current switching combination and the measuring of the voltage of the link circuit.

### Sensorless control using reduced Luenberger observer

A reduced observer is such observer which can be characterized by a lower order than the order of the system. In our case, after the reduction the number of state variables is equal to the number of output variables (two components), but the number of measured variables is higher (four components).

In sensorless control, observer processes matrix equations describing the behaviour of the PMSM. Reduced Luenberger observer reconstructs the state variables from the knowledge of the inputs and outputs of the system. The output of the observer is the induced voltage of the machine.

Figure 2 shows the different coordinate systems used for the mathematical description of the PMSM.

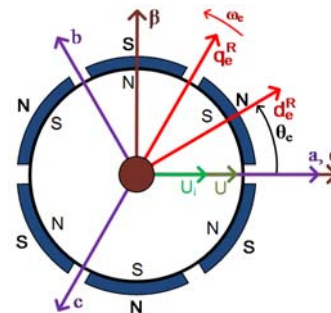


Fig.2. Representation of coordinate systems

The mathematical model can be expressed in matrix form in the coordinates  $\alpha, \beta$  (see equations 1, 2), which is a better alternative for the mathematical expression of the Luenberger observer [18].

$$(1) \begin{bmatrix} u_{S\alpha} \\ u_{S\beta} \end{bmatrix} = \begin{bmatrix} R_S + L_S \frac{d}{dt} & 0 \\ 0 & R_S + L_S \frac{d}{dt} \end{bmatrix} \cdot \begin{bmatrix} i_{S\alpha} \\ i_{S\beta} \end{bmatrix} + K_E \omega_e \begin{bmatrix} \cos \theta_e \\ \sin \theta_e \end{bmatrix} \mathbf{u}_i$$

$$(2) \begin{bmatrix} u_{i\alpha} \\ u_{i\beta} \end{bmatrix} = K_E \omega_e \begin{bmatrix} \cos \theta_e \\ \sin \theta_e \end{bmatrix}, \quad \frac{d}{dt} \begin{bmatrix} u_{i\alpha} \\ u_{i\beta} \end{bmatrix} = \begin{bmatrix} 0 & -\omega_e \\ \omega_e & 0 \end{bmatrix} \cdot \begin{bmatrix} u_{i\alpha} \\ u_{i\beta} \end{bmatrix}$$

By combining and adjusting these equations we get the full matrix model of the SMPM for the observer.

$$(3) \frac{d}{dt} \begin{bmatrix} \dot{\mathbf{x}} \\ i_{S\alpha} \\ i_{S\beta} \\ u_{i\alpha} \\ u_{i\beta} \end{bmatrix} = \begin{bmatrix} \mathbf{A} & \mathbf{0} \\ \mathbf{0} & \mathbf{B} \end{bmatrix} \cdot \begin{bmatrix} \mathbf{x} \\ i_{S\alpha} \\ i_{S\beta} \\ u_{i\alpha} \\ u_{i\beta} \end{bmatrix} + \begin{bmatrix} \mathbf{0} \\ \mathbf{0} \\ \mathbf{0} \\ \mathbf{0} \\ \mathbf{0} \end{bmatrix} \cdot \begin{bmatrix} \mathbf{u} \\ u_{S\alpha} \\ u_{S\beta} \end{bmatrix}$$

We define the state space and the state vector:

$$(4) \dot{\mathbf{x}} = \mathbf{Ax} + \mathbf{Bu} \quad \text{where } \mathbf{x} = [i_{S\alpha} \ i_{S\beta} \ u_{i\alpha} \ u_{i\beta}]^T \\ \mathbf{y} = \mathbf{Cx} + \mathbf{Du}$$

For the case when the state vector contains the measured quantities, reduced form of the Luenberger observer can be used. The aim is to obtain the state vector that contains only two components of the induced voltage and to simplify the observer. Therefore, we modify equations (1, 2) as follows:

$$(5) \frac{d}{dt} \begin{bmatrix} \mathbf{x}_n \\ \mathbf{x}_u \end{bmatrix} = \begin{bmatrix} A_{11} & A_{12} \\ A_{21} & A_{22} \end{bmatrix} \cdot \begin{bmatrix} \mathbf{x}_n \\ \mathbf{x}_u \end{bmatrix} + \begin{bmatrix} B_1 \\ B_2 \end{bmatrix} \mathbf{u}$$

$$\mathbf{y} = [\mathbf{I} \ 0] \cdot \begin{bmatrix} \mathbf{x}_n \\ \mathbf{x}_u \end{bmatrix}$$

$$(6) \mathbf{x}_n = [i_{S\alpha} \ i_{S\beta}]^T \\ \mathbf{x}_u = [u_{i\alpha} \ u_{i\beta}]^T$$

where:  $\mathbf{x}_n$  is vector of measurable quantities and  $\mathbf{x}_u$  is vector of immeasurable quantities.

The reduced form of the Luenberger observer can be created from the theory of the classical Luenberger observer

according to [18]. State description and meaning of individual matrices will be as follows:

$$(7) \quad \begin{aligned} \dot{\mathbf{z}} &= \mathbf{Dz} + \mathbf{Fi} + \mathbf{Gu} \\ \dot{\mathbf{x}}_{\mathbf{u}} &= \mathbf{z} + \mathbf{Li} \\ \mathbf{z} &= \begin{bmatrix} z_1 \\ z_2 \end{bmatrix}, \mathbf{u}_{\mathbf{i}} = \begin{bmatrix} u_{i\alpha} \\ u_{i\beta} \end{bmatrix}, \mathbf{i} = \begin{bmatrix} i_{S\alpha} \\ i_{S\beta} \end{bmatrix}, \mathbf{u} = \begin{bmatrix} u_{S\alpha} \\ u_{S\beta} \end{bmatrix} \end{aligned}$$

$$(8) \quad \begin{aligned} \mathbf{G} &= -\mathbf{LB}_1 \\ -\mathbf{LA}_{11} + \mathbf{A}_{21} + \mathbf{DL} &= \mathbf{F} \\ -\mathbf{LA}_{12} + \mathbf{A}_{22} - \mathbf{D} &= \mathbf{0} \\ \mathbf{D} &= d_L \mathbf{[I]} = \begin{bmatrix} d_L & 0 \\ 0 & d_L \end{bmatrix} \end{aligned}$$

$$(9) \quad \begin{aligned} \mathbf{F} &= [-\mathbf{LA}_{11} + \mathbf{A}_{21} + \mathbf{DL}] = (R_S + d_L L_S) \begin{bmatrix} d_L & \omega_e \\ -\omega_e & d_L \end{bmatrix} \\ \mathbf{G} &= [-\mathbf{LB}_1 + \mathbf{B}_2] = -\begin{bmatrix} d_L & \omega_e \\ -\omega_e & d_L \end{bmatrix} \\ \mathbf{L} &= [-\mathbf{D} + \mathbf{A}_{22}] \mathbf{A}_{12}^{-1} = L_S \begin{bmatrix} d_L & \omega_e \\ -\omega_e & d_L \end{bmatrix} \end{aligned}$$

Last mathematical adjustment is necessary due to the implementation of the observer in the software Matlab-Simulink. This requires to enter the matrices of state space only in the traditional form, so the following equations (10)

$$(10) \quad \begin{aligned} \begin{bmatrix} \dot{z}_1 \\ \dot{z}_2 \end{bmatrix} &= \begin{bmatrix} d_L & 0 \\ 0 & d_L \end{bmatrix} \cdot \begin{bmatrix} z_1 \\ z_2 \end{bmatrix} + \\ &+ (R_S + d_L L_S) \begin{bmatrix} d_L & \omega_e \\ -\omega_e & d_L \end{bmatrix} \cdot \begin{bmatrix} i_{S\alpha} \\ i_{S\beta} \end{bmatrix} - \begin{bmatrix} d_L & \omega_e \\ -\omega_e & d_L \end{bmatrix} \begin{bmatrix} u_{S\alpha} \\ u_{S\beta} \end{bmatrix} \\ \begin{bmatrix} u_{i\alpha} \\ u_{i\beta} \end{bmatrix} &= \begin{bmatrix} z_1 \\ z_2 \end{bmatrix} + L_S \begin{bmatrix} d_L & \omega_e \\ -\omega_e & d_L \end{bmatrix} \cdot \begin{bmatrix} i_{S\alpha} \\ i_{S\beta} \end{bmatrix} \end{aligned}$$

must be adapted to the form (11):

$$(11) \quad \begin{aligned} \dot{\mathbf{x}} &= \mathbf{Ax} + \mathbf{Bu} \\ \dot{\mathbf{y}} &= \mathbf{Cx} + \mathbf{Du} \\ \mathbf{u} &= \begin{bmatrix} i_{S\alpha} \\ i_{S\beta} \\ u_{S\alpha} \\ u_{S\beta} \end{bmatrix}, \mathbf{x} = \begin{bmatrix} x_{\alpha} \\ x_{\beta} \end{bmatrix}, \mathbf{y} = \begin{bmatrix} u_{i\alpha} \\ u_{i\beta} \end{bmatrix} \\ \mathbf{A} &= \begin{bmatrix} d_L & 0 \\ 0 & d_L \end{bmatrix} \\ \mathbf{B} &= \begin{bmatrix} d_L (R_S + d_L L_S) & \omega_e \cdot (R_S + d_L L_S) & -d_L & -\omega_e \\ -\omega_e \cdot (R_S + d_L L_S) & d_L (R_S + d_L L_S) & \omega_e & -d_L \end{bmatrix} \\ \mathbf{C} &= \begin{bmatrix} 1 & 0 \\ 0 & 1 \end{bmatrix} \\ \mathbf{D} &= L_S \begin{bmatrix} d_L & \omega_e & 0 & 0 \\ -\omega_e & d_L & 0 & 0 \end{bmatrix} \end{aligned}$$

Now we have the final equations that will be used in the simulation. The parameter  $d_L$  is used to set the observer, respectively, indicates a compromise between the speed and accuracy.

#### Processing of the observer output signals

In the previous text, it was already mentioned, that the observer produces at its outputs information about the actual value of the induced voltage. It can be distorted by

an offset that needs to be eliminated. In the mathematical model of the machine, derivative is used for removing slowly varying DC signal. It is not necessary to use the limiter, because the observer does not create output signals with high steepness. Then it is possible to apply the function  $\arctan2$  for calculation of the rotor position (see eq. 12).

$$(12) \quad \theta_{e\_est} = \arctan2\left(\frac{u_{i\beta}}{u_{i\alpha}}\right)$$

The difference with function  $\arctan$  can be found only in changing the field of values from the interval  $[-0.5\pi, 0.5\pi]$  to range  $[-\pi, \pi]$ . However, the previous applies only for the positive motor speed. At negative speed, the constant  $\pi$  must be added to the actual rotor position.

The angular speed of the motor can be obtained by derivation of the rotor position. However, it is necessary to adjust the signal, because obtained quantity is very noisy.

A better variant, which was also used in the simulation, is to calculate the speed from actual values of the two components of induced voltage (see equation 13).

$$(13) \quad \omega_{e\_est} = \frac{1}{K_E} \sqrt{(u_{i\alpha})^2 + (u_{i\beta})^2} \operatorname{sign}\left(\frac{d\theta_{e\_est}}{dt}\right)$$

However, it should be noted that this method can calculate only the size of the speed. Its direction is necessary to find another way. As can be seen the direction of the signal speed is very important because it is necessary for the estimation speed and angular position. The first variant for obtaining this signal is to determine it from the derivative sign (see equation 13).

The second alternative for obtaining the direction of rotation, which we have designed, uses the principle that at direction changing, both components of the induced voltage must pass through zero.

#### Laboratory workplace

To verify the simulation models and principles as well as sensorless vector control, experimental laboratory workplace with the PMSM supplied by low voltage was created. The basic parts are machine set, frequency converter, control system with DSP, personal computer and the necessary measuring instruments. The specifications of the PMSM utilizing in this research are listed in Table 1.

The motor parameters have been chosen with regard to the application in a small electric car. Because of battery power, voltage in DC link of the voltage inverter is low and the output currents of the PMSM are significant. The PMSM was designed so that it can be powered from a battery with voltage 48 V. The PMSM is powered by a frequency converter made at the Department of Electronics. Switching elements are IGBT. The switching frequency is 10 kHz. LEM SA sensors are used for current measurement.

Table 1. The parameters of the PMSM

Rated voltage	30 V
Voltage of DC link	48 V
Rated current	34 A
Maximal current	224 A
Rated power	160 W
Rated torque	4.6 Nm
Maximal torque	21 Nm
Rated speed	3000 rpm
Maximal speed	12000 rpm
Number of pole-pairs	3
Voltage constant	0.0086 V/rpm
Torque constant	0.14 Nm/A
Stator resistance	0.05 $\Omega$
Stator inductance	0.30 mH
Moment of inertia	2.7 kgcm <sup>2</sup>

In the control system, a Freescale DSP 56F8037 digital signal processor is used. The base board with the DSP also

contains a transducer of the serial line to USB; therefore, communication and data acquisition uses the USB interface. The program is loaded and tuned via the USB interface with a USB TAP by Freescale.

### Experimental results

The quality of estimation and behaviour of the sensorless controlled drive with reduced Luenberger observer were experimentally tested.

The experimental results are shown in the following Figures 3 to 6 which show the time courses of characteristic variables that were measured on the laboratory stand of the AC drive with sensorless control. Estimated and measured signals are presented in respective color of their variables. In the case of the estimated variables, there are the speed  $\omega_{m\_est}$ , rotor position  $\Theta_{e\_est}$  and direction of rotation  $\omega_{dir}$  (the sign of this variable is the direction of rotation). Measured signals from the incremental encoder are speed  $\omega_m$  and rotor position  $\Theta_e$ . The signals from the current sensors are presented in orthogonal coordinate system  $d, q$  coupled with the flux of the permanent magnets [19].

In Figure 3, we can see of time responses of selected quantities at reversing AC drive speed -1000  $\rightarrow$  +1000 rpm.

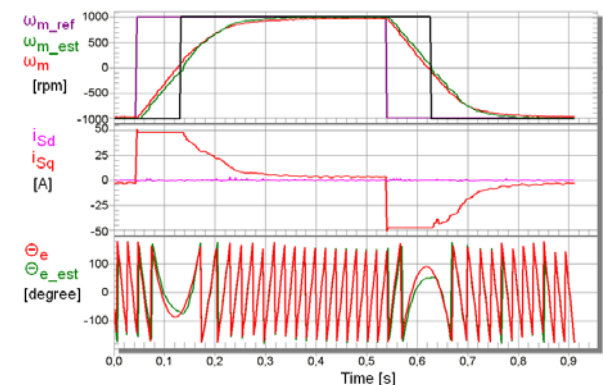


Fig.3. Reversing at sensorless control

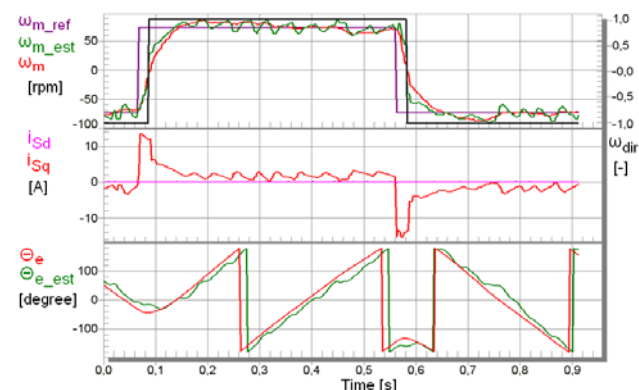


Fig.4. Reversing at sensorless control

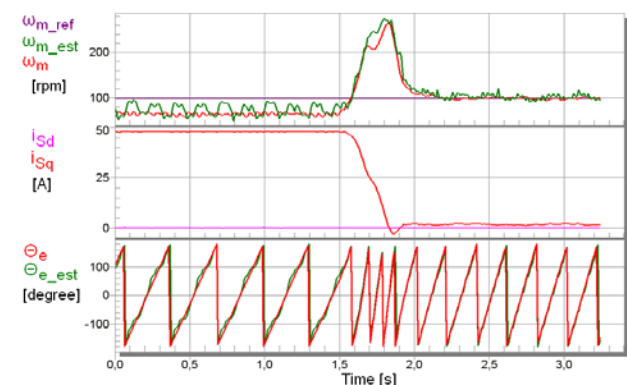


Fig.5. Response of the AC drive with the observer at load disconnection

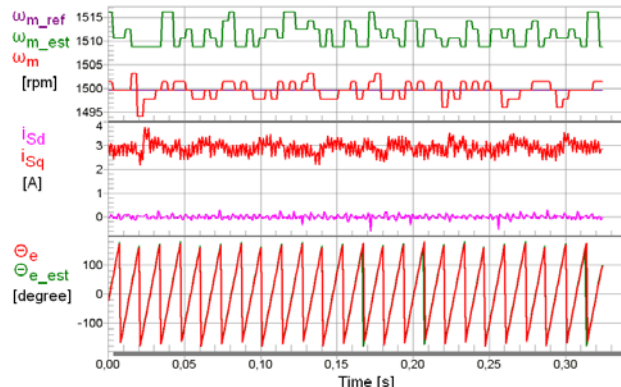


Fig.6. AC drive operation at steady state

In the case of sensorless control at low speeds we can see that the estimation accuracy decreases and oscillation appears, which is more significant at the calculated speed, but is evident in estimated rotor position (see Fig. 4). These inaccuracies are given in particular by the measured voltage signals from which the speed is then determined. An involvement of the estimated values into control feedback causes oscillation in the torque current component  $i_{Sq}$ .

Problems are caused by variable impedance of the machine, current control, nonlinearities of the voltage inverter (dead time and voltage drops on the switching elements), variable DC link voltage (current peaks) and by many other factors.

The sensorless method presented in this paper has a minimum speed at which the motor is able speed reversing around 60 rpm (see Fig. 4).

Behaviour of the AC drive at low speed and with the load is shown in Figure 5. We can see the speed overshoot in response to load change at the sensorless control with the observer and at reference speed 100 rpm.

Due to the fact that the PMSM has set the current limit of both current components to the nominal value, it can only give a maximum rated torque. We can see that the load was greater than nominal torque because the motor has not reached the desired speed.

AC drive running at steady state was measured at different speeds and time courses of variables are presented on the next figure (see Fig. 6). The presented Fig. 6 is suitable for assessing the quality of estimation during vector control of AC drive. We can see that the absolute error has a value about 13 rpm at 1500 rpm, which corresponds to a relative error 0.86%. The value is worse at low speeds, where the error is about 5%.

### Conclusion

The article is focused on sensorless control method based on the mathematical model of the machine using the reduced Luenberger observer. For the simulation and experimental verification, the synchronous motor with the permanent magnets located on the surface of the rotor was selected, which is suitable for the drive unit of small electric cars. Practical benefit for technical practice is the application of the PMSM vector control in the small electric car CityEI.

The article contains the experimental results which were obtained by measurement on the laboratory stand with the AC drive. The sensorless controlled drive can be compared with vector controlled drive on which the observer runs simultaneously.

The article also shows that the sensorless control can be realized with 16-bit digital processing, measurement with accuracy 12 bits and processing power 32 MIPS. For easy and simple control of the AC drive, an interface of

FreeMaster program can be used. The interface allows switching between the sensor and sensorless control and choosing various automatic modes such as reversing, changing speed, changing torque, etc.

Range of desired drive speed is limited. The upper limit is determined by the DC link voltage for which the machine is designed, if we do not consider weakening. The minimal speed is determined by the stability of the sensorless control. Below this value, the system is not observable. The minimal value of speed approximately 60 rpm was determined by experiment. At this value, the drive is also able to reverse with the load. Let us emphasize that the PMSM in this case is supplied by voltage lower than 1 V.

The development of various sensorless methods is very dynamic. Despite this fact, today does not exist one way of sensorless control, which would cover the entire speed and power range of electrical controlled drives. For low and zero speed, different methods are suitable which use the principle of the signal injection. However, these methods have specific disadvantages such as torque ripple, acoustic noise and require machines with large difference in the longitudinal and transverse inductance. In contrast, the methods based on the mathematical model do not have these disadvantages, but the minimum operating speed is restricted. Some of the hybrid sensorless control method combining the mathematical model and the signal injection could be applicable at the end of the sensorless control development.

#### List of used symbols

$\mathbf{x}^S$	quantity defined in stator coordinate system $[\alpha, \beta]$
$\mathbf{x}^R$	quantity defined in rotor coordinate system $[d, q]$
$U_{S\alpha}, U_{S\beta}$	components of the stator voltage vector in coordinate system $[\alpha, \beta]$
$U_{i\alpha}, U_{i\beta}$	components of the induced voltage vector in coordinate system $[\alpha, \beta]$
$U_{i\alpha\beta\_est}$	estimated components of the induced voltage vector in coordinate system $[\alpha, \beta]$
$i_{S\alpha}, i_{S\beta}$	components of the stator current vector in coordinate system $[\alpha, \beta]$
$i_{Sd}$	magnetizing current component in $[d, q]$ system
$i_{Sq}$	torque current component in $[d, q]$ system
$i_{Sd\_ref}, i_{Sq\_ref}$	reference magnetizing and torque component of stator current vector
$d_L$	parameter of Luenberger observer
$K_E$	voltage constant of the PMSM
$R_S$	stator resistance
$L_S$	stator inductance
$L_d$	inductance in the longitudinal axis of the rotor
$L_q$	inductance in the transverse axis of the rotor
$\theta_e$	rotor angle
$\theta_{e\_est}$	estimated rotor angle
$\omega_e$	electrical rotor angular speed
$\omega_{e\_est}$	estimated electrical rotor angular speed
$\omega_{m\_ref}$	reference rotor angular speed
$\omega_m$	real rotor angular speed
$\omega_{m\_est}$	estimated rotor angular speed

#### Acknowledgment

The article has been elaborated in the framework of the IT4Innovations Centre of Excellence project, reg. no. CZ.1.05/1.1.00/02.0070 funded by Structural Funds of the European Union and state budget of the Czech Republic and in the framework of the project SP2013/118 which was supported by Student Grant Competition of VSB-TU of Ostrava.

#### REFERENCES

[1] Li Yongdong, Zhu Hao, Sensorless control of permanent magnet synchronous motor - a survey, in *proceedings of IEEE Vehicle Power and Propulsion Conference (VPPC)*, pp. 1-8, Harbin, China, 2008.

[2] Gieras F. J., Wing M., Permanent Magnet Motor Technology: Design and Applications, CRC Press, 2002.

[3] Glinka T., Krol E., Bialas A., Wolnik T., Axial Flux Permanent Magnet Motors as Drive Slow Moving Vehicles - Review of Construction, *Przeglad Elektrotechniczny*, Vol. 87, N. 3, pp. 1-4, 2011.

[4] Vas P., Sensorless Vector and Direct Torque Control, Oxford University Press, 1998.

[5] Lin Ch. H., A Novel Hybrid Recurrent Wavelet Neural Network Control for a PMSM Drive Electric Scooter Using Rotor Flux Estimator, *International Review of Electrical Engineering - IREE*, Vol. 7, N. 3, pp. 4486-4498, 2012.

[6] Kaminski M., Dybkowski M., Analysis of the Sensorless Vector Control of Induction Motor With MRAS(CC) Estimator and Neural Model Applied for Speed Calculation, *Przeglad Elektrotechniczny*, Vol. 88, N. 4B, pp. 116-121, 2012.

[7] Perdukova D., Fedor P., Simple Method of Fuzzy Linearization of Non-Linear Dynamic System, *Acta Technica CSAV*, Vol. 55, N. 1, pp. 97-111, 2010.

[8] Biskup T., Initial rotor position estimation of permanent magnet synchronous machine, *Przeglad Elektrotechniczny*, Vol. 88, N. 4A, pp. 157-162, 2012.

[9] Dhaouadi R., Mohan N., Norum L., Design and Implementation of an Extended Kalman Filter for the State Estimation of a Permanent Magnet Synchronous Motor, *IEEE Transactions on Power Electronics*, Vol. 6, pp. 491-497, 1991.

[10] Daubaras A., Zilyls M., Vehicle Detection based on Magneto-Resistive Magnetic Field Sensor, *Electronics and Electrical Engineering*, No. 2(118), pp. 27-32, 2012.

[11] Abdi B., Bahrami H., Ghiasi M. I., Ghasemi R., PM Machine Optimization in Variable Speed EMB Application, *International Review of Electrical Engineering - IREE*, Vol. 7, N. 3, pp. 4412-4418, 2012.

[12] D. Uzel, Peroutka Z., Optimal Control and Identification of Model Parameters of Traction Interior Permanent Magnet Synchronous Motor Drive, in *proceedings of 37th Annual Conference of the IEEE Industrial-Electronics-Society (IECON)*, pp. 1960-1965, Melbourne, 2011.

[13] Vittek J., Bris P., Makys P., Stulrajter M., Forced dynamics control of PMSM drives with torsion oscillations, *The International Journal for Computation and Mathematics in Electrical and Electronic Engineering COMPEL*, Vol. 29, Issue 1, pp. 187-204, 2010.

[14] Tudorache T., Popescu M., Optimal Design Solutions for Permanent Magnet Synchronous Machines, *Advances in Electrical and Computer Engineering Journal*, Vol. 11, No. 4, pp. 77-82, 2011.

[15] Jansen P. L., Lorenz R. D., Transducerless Position and Velocity Estimation in Induction and Salient AC Machines, *IEEE Transactions on Industry Applications*, Vol. 31, pp. 240-247, 1995.

[16] Linke M., Kennel R., Holtz J., Sensorless speed and position control of synchronous machines using alternating carrier injection, in *proc. of IEEE International Electric Machines and Drives Conference - IEMDC'03*, Vol. 2, pp. 1211- 1217, 2003.

[17] Tudorache T., Trifu I., Ghita C., Bostan V., Improved Mathematical Model of PMSM Taking Into Account Cogging Torque Oscillations, *Advances in Electrical and Computer Engineering*, Vol.12, No 3, pp. 59-64, 2012.

[18] Kim J. K., Sul S. K., High Performance PMSM drives without Rotational Position Sensors Using Reduced Order Observer, in *proceedings of Industry Applications Conference*, pp. 75-82, Orlando, USA, 1995.

[19] Rech P., Sensorless Control of AC Controlled Drive with Permanent Magnet Synchronous Motor, PhD. Thesis, VSB-Technical University of Ostrava, 2010.

**Authors:** Prof. Ing. Pavel Brandstetter, VSB-Technical University of Ostrava, Faculty of Electrical Engineering and Computer Science, Department of Electronics, 17.listopadu 15, 70833 Ostrava-Poruba, Czech Republic, E-mail: [pavel.brandstetter@vsb.cz](mailto:pavel.brandstetter@vsb.cz).  
Ing. Pavel Rech, Ph.D., VSB-Technical University of Ostrava, Faculty of Electrical Engineering and Computer Science, Department of Electronics, 17.listopadu 15, 70833 Ostrava-Poruba, Czech Republic, E-mail: [pavel.rech@vsb.cz](mailto:pavel.rech@vsb.cz).